energies

MDPI

Article

A Comparative Analysis on the Variability of Temperature Thresholds through Time for Wind Turbine Generators Using Normal Behaviour Modelling

Alan Turnbull [1,*], James Carroll [1] and Alasdair McDonald [2]

[1] Institute of Energy and Environment, Electronic and Electrical Engineering, University of Strathclyde, Glasgow G1 1XQ, UK; j.carroll@strath.ac.uk
[2] Institute for Energy Systems, School of Engineering, University of Edinburgh, Edinburgh EH9 3DW, UK; alasdair.mcdonald@ed.ac.uk
* Correspondence: a.turnbull@strath.ac.uk

Abstract: Data-driven normal behaviour models have gained traction over the last few years as a convenient way of modelling turbine operational health to detect anomalies. By leveraging high-dimensional operational relationships, temperature thresholds can be automatically calculated based on each individual turbine unique operating envelope, in theory minimising false alarms and providing more reliable diagnostics. The aim of this work is to provide further insight into practical uses and limitations of implementing normal behaviour temperature models in practice, to inform practitioners, as well as assist in improving wind turbine generator fault detection systems. Results suggest that, on average, as little as two months of data are adequate to produce stable temperature alarm thresholds, with the worst case example requiring approximately 200–290 days of data depending on the component and desired convergence criteria.

Keywords: wind turbine; SCADA; machine learning; temperature; modelling; threshold; alarm

Citation: Turnbull, A.; Carroll, J. A Comparative Analysis on the Variability of Temperature Thresholds through Time for Wind Turbine Generators Using Normal Behaviour Modelling. *Energies* **2022**, *15*, 5298. https://doi.org/10.3390/en15145298

Academic Editor: Xiandong Ma, Sinisa Durovic, Mohamed Benbouzid and Davide Astolfi

Received: 10 May 2022
Accepted: 8 July 2022
Published: 21 July 2022

1. Introduction

As wind turbines continue to increase in size and capacity, wind farm availability also becomes increasingly important to reduce unplanned downtime and minimise lost production. One of the most promising ways to contribute to this goal of maximising availability is through advanced turbine monitoring and anomaly detection. The aim is to flag a range of issues allowing asset managers time to effectively plan and perform proactive maintenance activities.

Wind turbine behaviour is complex and is influenced by a variety of operational parameters including changing wind speed, direction, turbulence, temperature and humidity, as well as externally controlled actions such as curtailment. Techniques are required that can detect subtle changes in individual turbine behaviour over all expected operating regions to help detect anomalies and minimise false alarms. To this end, normal behaviour models (NBM) have gained interest in both academic research and industry.

1.1. Literature Review

Research published involving NBM's have been popular in recent years across various condition monitoring applications. The full process of developing a NBM will be discussed in later sections; however, the key principle behind NBMs is that they rely on empirically modelling a measured parameter during a training phase to set the boundaries of what is considered normal behaviour. The residual of the measured parameter minus the predicted modelled parameter is used as a fault indicator, with normal behaviour having residual values of approximately zero (±expected noise). Ref. [1] differentiated NBMs into two distinct categories; Full Signal ReConstruction (FSRC) and AutoRegressive with eXogenous

input modelling (ARX). The former uses only signals other than the target variable to predict the target variable, while the latter also makes use of the historical values of the target variable. This work will use the former, implementing a random forest regressive model. Ensemble methods in machine learning utilise multiple algorithms to gain more accurate and stable predictions than could be achieved with a single algorithm. Random forests can be considered an ensemble of decision trees, which aims to overcome some of the limitations of a single decision tree of overfitting and high variance [2].

Models in literature range from simple linear and polynomial fits such as [3], which used a linear ARX model to detect generator bearing failure by modelling bearing temperature and [4], which developed higher order polynomial FSRC models of drive train temperatures. Similar approaches have also been shown to detect faults of other wind turbine components such as transformers in [5]. To improve upon these modelling techniques, ANNs were introduced to capture nonlinear relationships between observations and increase model dimensionality, as demonstrated in [6] through detection of bearing damage in offshore wind turbines. In [7], it was demonstrated how ANNs could be used to detect main bearing damage three months before the turbine was stopped due to overheating by modelling main bearing temperature. ANNs' adaptability to different data was also shown in [8], where high frequency SCADA data was successfully used to detect bearing faults. Two back propagated Neural Networks (BPNNs) were used in [9], one to select relevant features, and the other to detect anomalies based on the RMSE between the measured and modelled target parameter. Other presented techniques include [10], which used a kNN algorithm to detect incipient failure in two turbines up to 6 months before failure. Nonlinear auto-regressive neural networks with exogenous inputs (NARX) models have recently been used in [11–13] to detect a range of gearbox component faults. Other research into fault detection using SCADA data include [14], which used a nonlinear state estimation technique to model gearbox behaviour, while probabilistic based methods were presented in [15].

Research involving data driven methods and high frequency vibration data has also been published extensively over the last decade in relation to wind turbine diagnostics. Unlike SCADA analysis, vibration signal analysis can make use of component kinematics and fault signatures to make a specific diagnosis. Much of the early work focused on wind turbine gearboxes due to reliability issues and contribution to turbine downtime; however, this has since extended to other drivetrain components such as generators, main bearings and blades. It was shown in [16] that diagnosis of gearboxes can be performed using time, frequency or time-frequency methods to analyse vibration signals. Methods to analyse the signal in the time domain have been proposed and are often based on statistical analysis methods to describe the time waveform such as peak value, RMS, kurtosis, mean, standard deviation and skewness. In lab conditions, this has proven to be a successful approach for both gearboxes [17] and generator bearings [18]. There are also many techniques using the frequency domain that have been proposed across different components and assemblies depending on specific fault signatures. The simplest of these is using Fast Fourier Transform, which looks at either the whole spectrum or specific frequency bands to extract features as demonstrated in [19]. When it comes to bearing diagnosis, Fast Fourier Transform is typically inadequate and requires more advanced signal processing techniques such as envelope analysis as shown in [20]. Regardless of the method used, once features have been extracted from the raw vibration signal, machine learning methods have proven to be a useful method of automatically classifying and detecting faults (as demonstrated above with SCADA data). An example is shown in [21], which employed an SVM classifier to successfully detect generator bearing faults. Gaussian Mixture Models (GMMs) were used in [22] to detect low speed bearing faults using both frequency and time domain features. A comparison of wind turbine gearbox vibration analysis algorithms based on feature extraction and classification can be found in [23,24].

Whilst no vibration data or associated analysis was used in this research, the applied machine learning techniques and modelling processes remain relevant. In an effort to

optimise CMS activities, a range of machine learning techniques are increasingly being used to enhance wind turbine diagnostics and prognostics, with multiple review papers now having been published over the last few years which can be found in [1,25,26]. In a review by Stecto et.al in 2018 [27], models were classified by typical ML steps, including data sources, feature selection and extraction, model selection (classification, regression), validation, and decision-making. Findings showed that most models use SCADA or simulated data, with almost two-thirds of methods using classification and the rest relying on regression.

1.2. Problem Statement

Although there has been research published showing the potential benefits of normal behaviour modelling, there is still much uncertainty over how much data are required. Papers typically utilise all available data to train and test the models, an approach that is understandable for turbines that have been operating for several years. The reason behind this approach is clear, providing that the wind turbine is operating under normal conditions, using more data makes it more likely that the model has captured all of the underlying relationships and expected variation. This in theory will allow for more accurate representation of normal behaviour, producing alarms thresholds that are set accurately to detect subtle changes in behaviour whilst minimising false flags.

In practice, this approach lends itself to established sites with many years of data to utilise, handpicking the most suitable data for training and validating the model. For new developments, however, where data are continuously being gathered from a zero starting position, this approach is not appropriate. Lots of questions remain about how to optimally train and develop models in this scenario. This paper aims to provide some insight into this by developing daily NBM's over the first year of a wind turbines life, analysing how temperature thresholds change over time across the generator for different turbines.

1.3. Paper Structure and Novelty

Section 2 outlines the methodology and data used throughout this research. This will provide details of the data itself, the machine learning algorithm used to build the NBM's, model inputs and outputs, model training, as well as how results were generated from the NBM that allowed thresholds to be compared through time. Section 3 presents the results, providing a comparison of temperature thresholds across different turbines and components within the generator. Finally, Section 4 presents the discussion and key conclusions drawn from the work.

The novelty of this work in the context of the wider research is as follows:

- Highlight the key similarities and differences between temperature thresholds produced from generator bearings and phase windings NBM's;
- Detail the variation in NBM temperatures thresholds observed across a fleet of the same turbine and component across different geographical locations;
- Provide insight into how temperature thresholds adapt over time as more data are introduced from the SCADA system.

2. Methodology and Data

2.1. Description of Raw Data

The SCADA data used for this analysis were obtained from 11 identical wind turbines with rated power of between 2–4 MW. The turbines each had a variable speed doubly-fed induction generator (DFIG), and were all within the first five years of operation at the time data were obtained. From the SCADA monitoring system, a total of 16 channels were made available associated with generator operation: the 10-min average, minimum, maximum and standard deviation of generator rotational speed and wind speed, the 10-min average generator bearing temperature, phase temperatures (1, 2 and 3), cooling water temperature and nacelle temperature, along with the 10-min average active power output from the generator. Continuous 10-min data were obtained for each turbine, which

gave approximately 52,560 data points per channel per turbine taking into consideration some variation of each individual turbine due to imperfect data coverage.

2.2. Methodology

The overall methodology described here will provide an overview of how alarm thresholds were generated from the raw SCADA timeseries. The process is shown in Figure 1, where the SCADA data are first of all separated by turbine. For each wind turbine, two NBM's are created: the first to model the generator bearing temperature and the second to model the generator winding temperature. Feature engineering involved normalising and analysing the data to understand the most relevant features to use for training. Common input features were used across both NBMs, each focused on an individual target feature as described above. Once features had been identified, data were then split into 365 progressive sub-datasets each having an additional 1 day of data. This was done to simulate a new wind farm site, for which more data would be continuously gathered and made available for training over the course of a year. For example, on sub-dataset 35, the model is trained with 35 days of data (or approximately 5040 data samples per feature), whereas, on sub-dataset 140, the model is trained with 140 days of data (or approximately 20,160 data samples). For each of the bearing and winding temperature NBM, several temperature thresholds were calculated each week based on the distribution of error residuals. This is the difference between predicted target temperature and measured target temperature; however, more detail will be provided in later sections about this process. Once thresholds had been established, they could be compared through time.

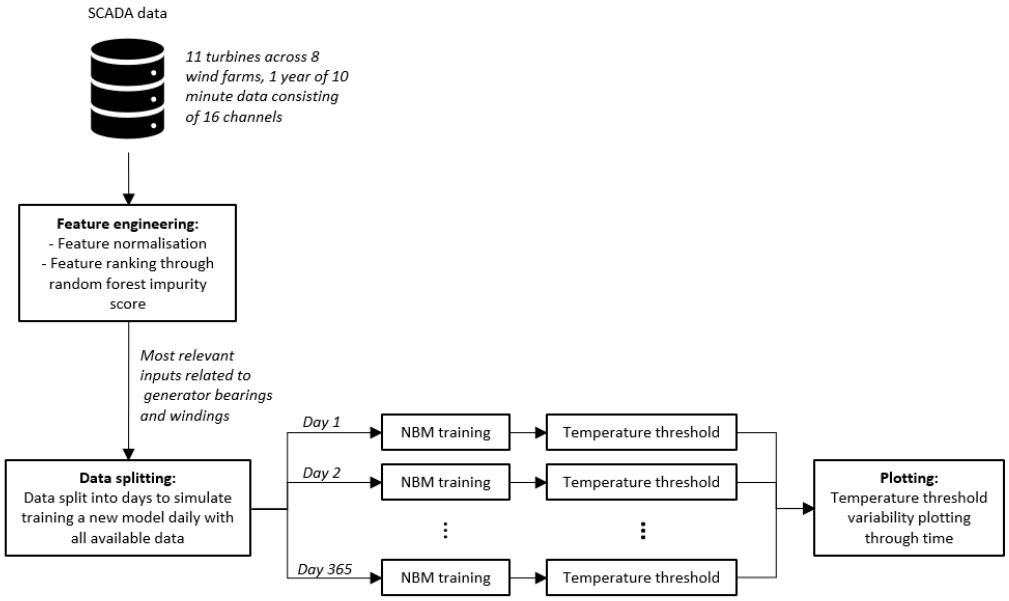

Figure 1. Methodology for generating NBM temperature threshold.

2.3. Feature Engineering

First of all, let us consider the power curve in relation to the two component temperatures that are to be monitored through a NBM. In Figure 2, (a) shows the power curve in relation to the generator bearing temperature, while (b) shows the same plot for the generator phase temperature. Note that the raw features have been cleaned to remove all data gathered while the turbine had a power output of below zero, and then normalised between 0–1.

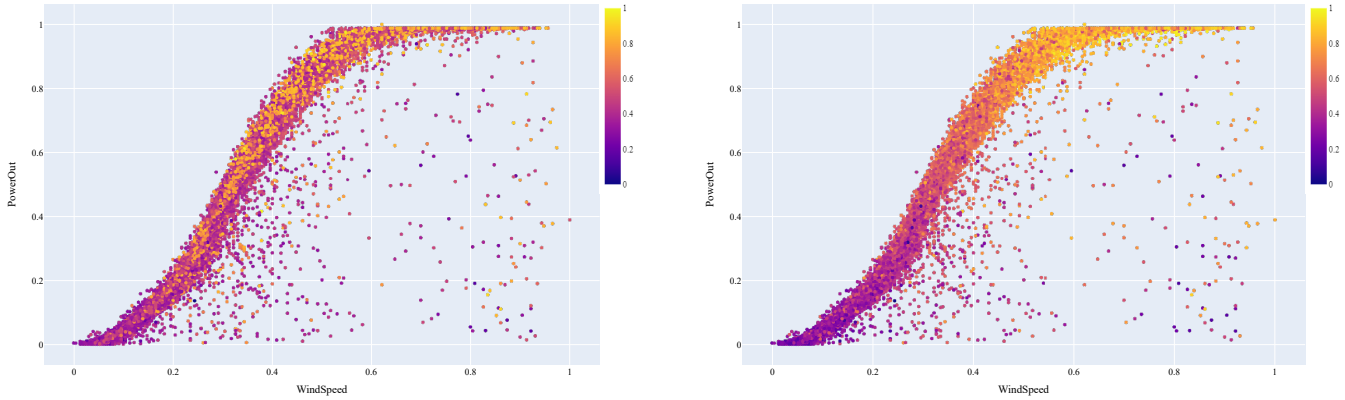

(a) Power curve - Generator bearing temperature (b) Power curve - Generator phase temperature

Figure 2. Power curves.

It can be seen that the 10-min. average phase temperature more closely correlates with the average power and wind speed. This is further emphasised in Figure 3, where (a) shows the direct relationship between the average generator bearing temperature, wind speed and power output over the same time period. One of the most obvious observations is the more complex relationship between generator bearing and both operating parameters, where two distinct relationships appear to be present. The turbine used does not have two generators (like some earlier models), nor is there any substantial periods of curtailment which may contribute to this temperature distribution (as seen in the power curve). One possible explanation could be in relation to the cooling system; however, with the data provided, it is impossible to state the cause conclusively. Conversely, the observed relationship between operating parameters and average generator phase temperature is relatively simple and linear.

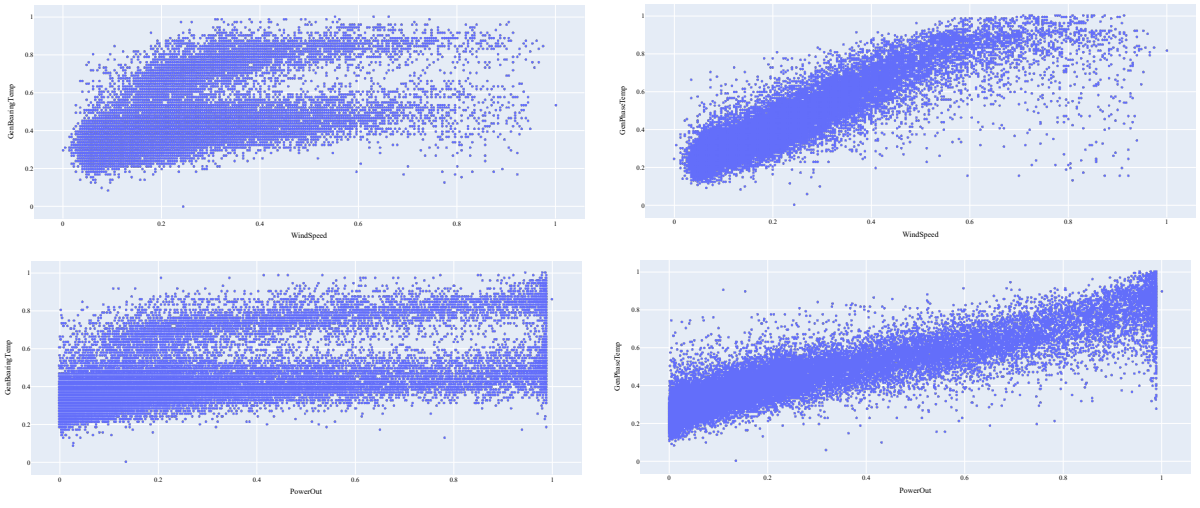

(a) Generator bearing temperature (b) Generator phase temperature

Figure 3. Relationship between component temperature and operating condition.

There are several ways to quantitatively assess feature importance for training a regressive model. One technique is univariate analysis, for which we can examine each feature individually to determine the strength of the relationship with the target variable. This can be useful to disregard irrelevant features which are noisy or uncorrelated, or conversely where inputs are heavily correlated and provide no additional information. For

example, one common metric to understand the relationship is the Pearson correlation coefficient, which measures the linear correlation between two variables. Figure 4 shows the Pearson coefficient for the input features described previously. The r value has a range of between −1 and 1, with two features showing total positive correlation if r = 1 and true negative correlation when r = −1. Two features will be completely uncorrelated if r = 0.

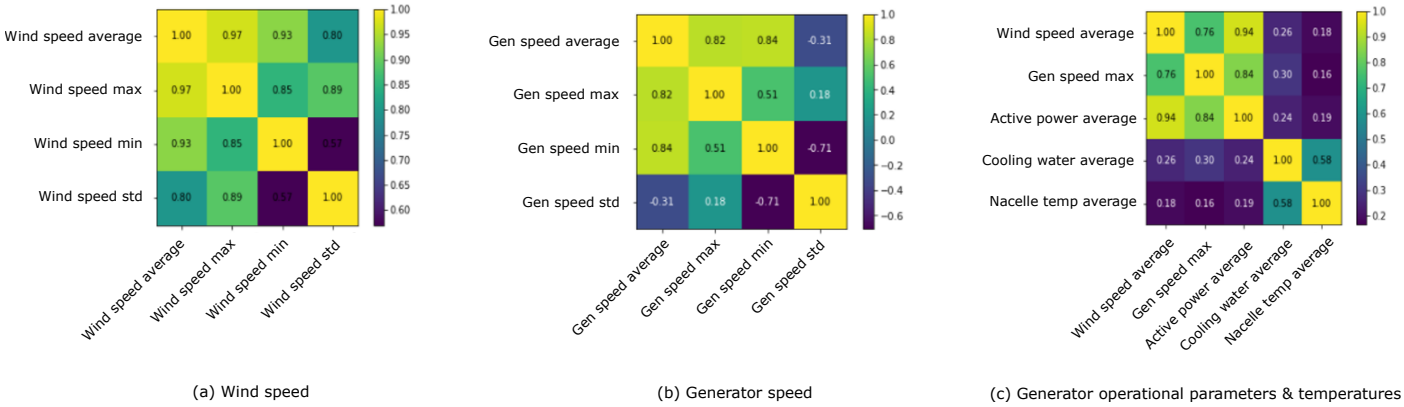

(a) Wind speed (b) Generator speed (c) Generator operational parameters & temperatures

Figure 4. Pearson coefficient for assessing linear correlation.

From the data inputs available, we see high positive correlation scores between average wind speed value and its distribution around the mean. The same can be said for generator speed when considering the maximum and minimum, although with more random standard deviation. With regard to operating parameters and surrounding temperatures, high correlation between power, wind speed and generator speed is observed. Cooling water temperature and nacelle temperature are not correlated linearly to turbine operation, although they are somewhat correlated to each other. Although useful, these metrics are quite restrictive and are not suitable for ranking high dimensional nonlinear relationships. To navigate this issue, another useful way to rank features is through a model based approach. For ease of application, a tree based model was used and involves training a random forest model and assessing feature importance based on the average decrease in impurity across all decision trees in the forest. As this is automatically computed during the training phase, it offers a convenient approach to assessing feature importance when dealing with nonlinear relationships. Feature importance of inputs in relation to NBM 1 (generator bearing temperature) and NBM 2 (generator phase winding temperature) are presented in Figure 5a and 5b, respectively.

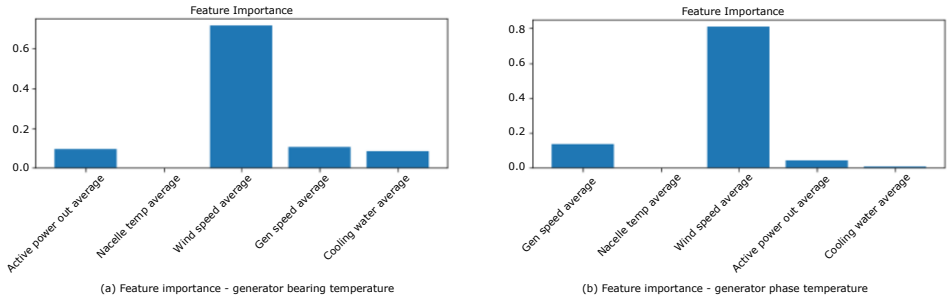

(a) Feature importance - generator bearing temperature (b) Feature importance - generator phase temperature

Figure 5. Overall feature importance of inputs and target using random forest impurity score.

In both cases, the most important feature was wind speed by a significant margin. Generator speed and power output provide the next level of importance in both models, with the cooling water temperature only significant when modelling the generator bearing. For both NBM 1 and 2, nacelle temperature was of zero importance. Based on the information presented above, Table 1 summarises the features used to train the NBM's. This consisted of the average active power output, wind speed, generator speed and cooling water temperature.

Table 1. SCADA channels used for NBM development.

SCADA Channel	Description	Model Feature	NBM
P_{output}	Average Active Power Output	Input	1, 2
$U_{generator}$	Average Generator Speed	Input	1, 2
U_{wind}	Average Wind Speed	Input	1, 2
$T_{nacelle}$	Average Generator Cooling Water Temperature	Input	1, 2
$T_{bearing}$	Average Generator Bearing Temperature	Target	1
T_{phase}	Average Generator Phase Winding Temperature	Target	2

2.4. NBM Description

The model used for this case study was a random forest regressive model, with the model predictors and response features highlighted in Table 1. Features were chosen based on the feature analysis described in the previous section. Model hyperparameters were determined through model testing and validation processes. Key hyperparameter values included: max tree depth of 4, number of tree estimators of 10, minimum samples per split of 2, with the quality of split measured by the mean squared error (MSE).

2.5. Alarm Generation

The process of actually generating the alarms from the target and input features can be found in Figure 6. This has been adapted from the conventional NBM development process published in [1,3]. As the regressive based NBM requires supervised learning, a training dataset consisting of inputs features $x(t)$ and target feature $y(t)$ is necessary. Once trained, the available input features can be used to generate predictions of expected target feature, $\hat{y}(t)$. This model prediction is then subtracted from the actual target feature recorded (in this case from the temperature sensor) to give the error residual $e(t)$. From here, the distribution of the error over the training period can be analysed. For this analysis, four percentiles of the distribution were investigated, P_{99}, P_{97}, P_{95} and P_{90}, which were the 99th, 97th, 95th and 90th percentiles, respectively. To convert these percentiles back into absolute values, they were added to the model prediction to create alarm thresholds A_{99}, A_{97}, A_{95} and A_{90}.

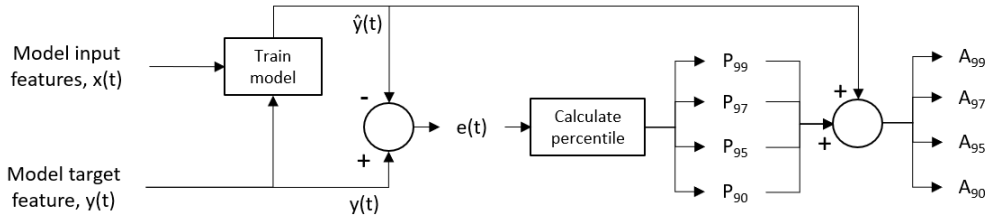

Figure 6. Process for creating alarm level through NBM, adapted from [1,3].

3. Results

3.1. Comparison of Alarm Thresholds through Time

Results will be presented for both NBM 1 and 2, representing the generator bearing temperature and generator phase winding temperature, respectively. For each day of the year, as described in Figures 1 and 6, four alarm thresholds were calculated based on different percentiles of the NBM error residuals. Plots showing the alarm thresholds changing through time are presented in Figure 7: (a) for bearing temperature and (b) for phase winding temperature.

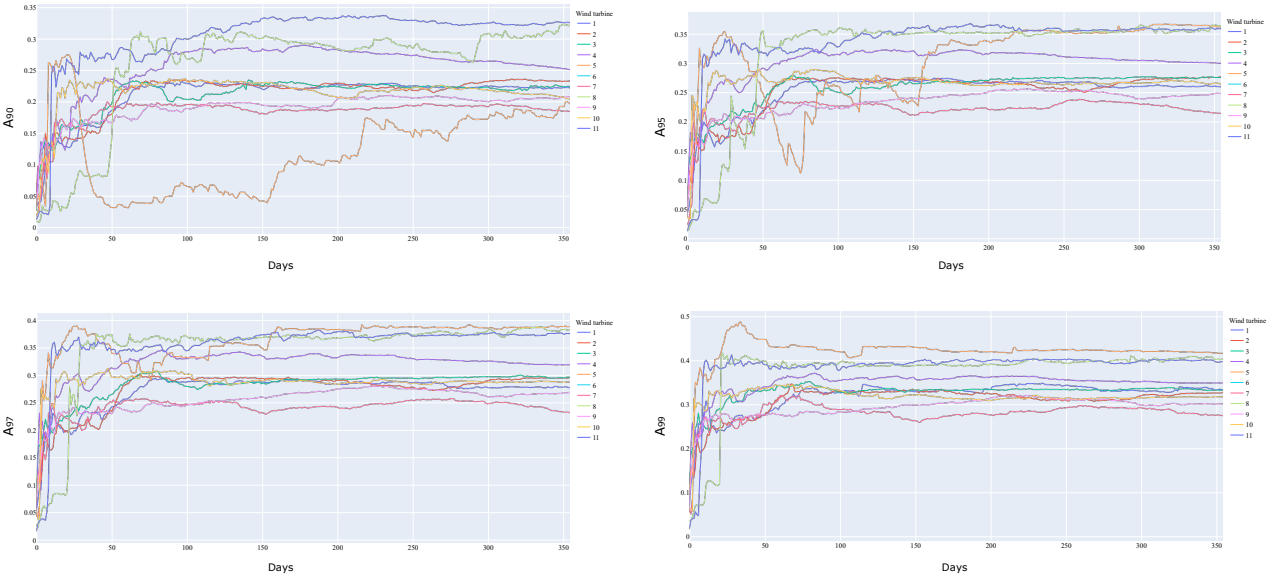

(**a**)

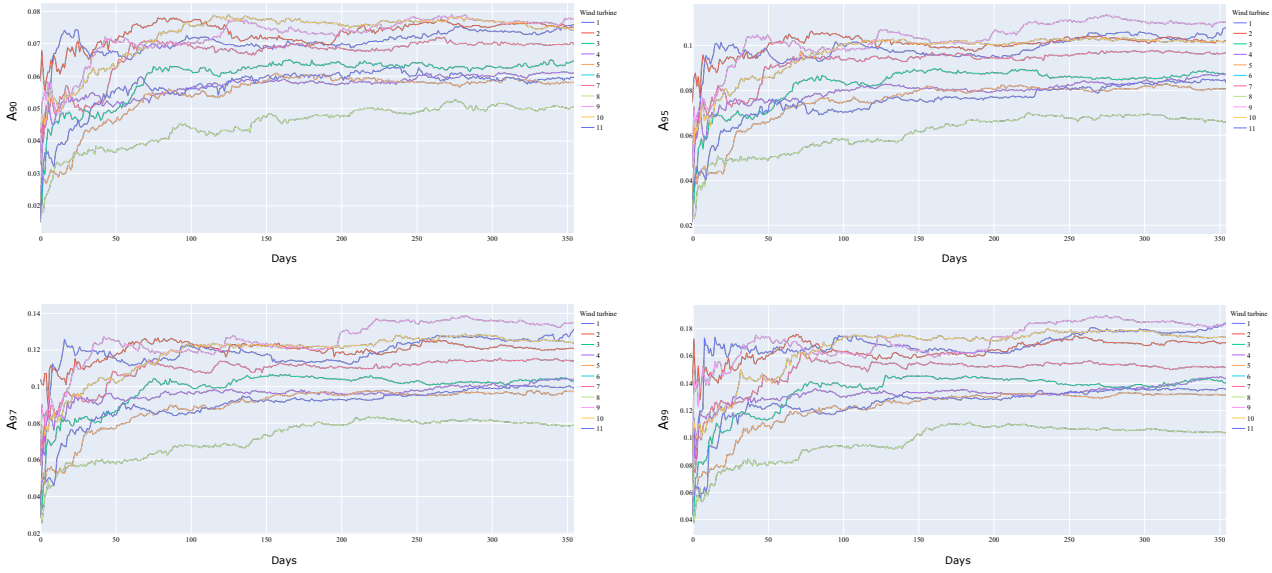

(**b**)

Figure 7. Temperature alarm thresholds calculated through time. (**a**) generator bearing temperature alarm; (**b**) generator phase winding temperature alarm.

For each NBM alarm threshold, we see variability between turbines both in time taken to converge and in absolute value after convergence. In terms of absolute values, Figure 8 shows the variation between turbines after convergence. For each turbine, the average of the final three values of each temperature threshold was used to create box plots for direct comparison.

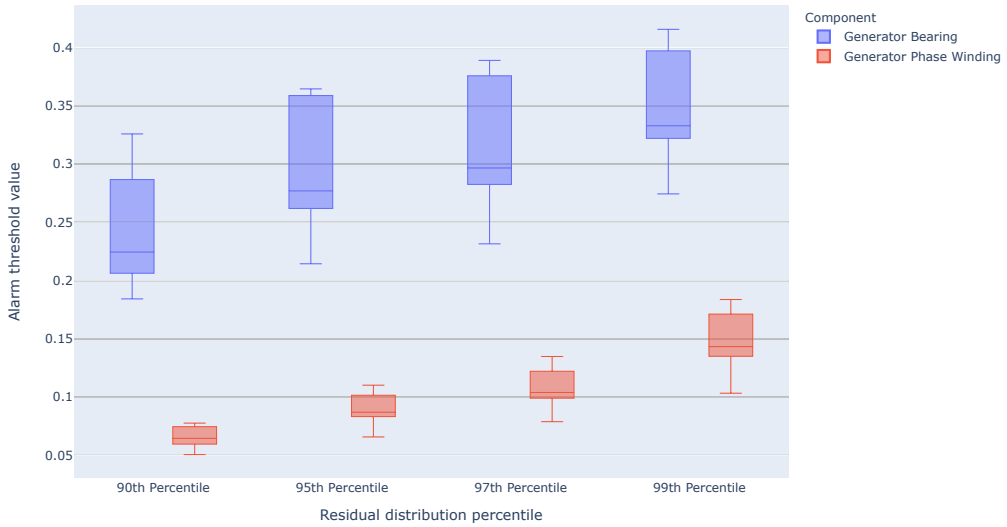

Figure 8. Variation in alarm threshold between turbines after convergence.

First of all, we see a much lower alarm threshold value for the generator winding in comparison to the bearing on average. Additionally, as expected due to the error distribution, a general increase is also observed as the higher percentile is used. With regard to variation between turbines, there was larger variation in the generator bearing thresholds compared to the phase windings. For the bearings, the variation between turbines was fairly consistent for each percentile; however, the windings showed increased variation when higher percentiles were used.

3.2. Alarm Threshold Convergence

Convergence is used in this instance as a measure of how much data are required for the model to produce consistent alarms and hence capture the expected variability of turbine normal behaviour. A more convenient way to visualise this is by looking at the rate of change of the alarm, which will settle around zero as the threshold converges. Figure 9 shows the daily change in temperature threshold:

$$dA = \frac{A_x - A_{(x-1)}}{A_n} \tag{1}$$

where dA is the percentage change in alarm level relative to the final converged threshold A_n, and A_x is the normalised alarm level for data sample x of dataset with length n.

For each of the two NBM's shown in Figure 9a,b, threshold convergence of 2%, 3%, 4% and 5% were considered across all alarm percentiles. Results are presented in Figure 10 and showed significant variation between turbines, even when considering the same alarm percentile and convergence criteria. In general, it was found that decreasing the convergence percentage from 5% to 2% led to longer convergence times. This would be expected due to tighter convergence constraints. The average convergence time based on 3% was between 50–60 days, with the majority of turbines not requiring more than 120 days, or approximately four months of data. These times significantly increased when using the 2% convergence criteria, which will be discussed in more detail during the next section.

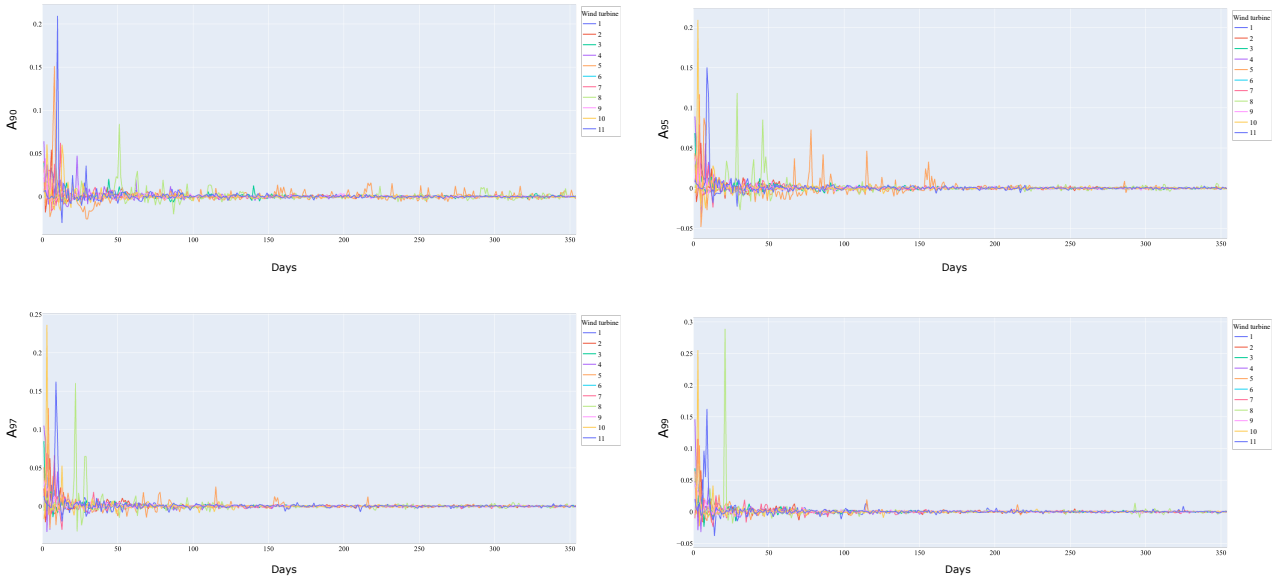

(**a**)

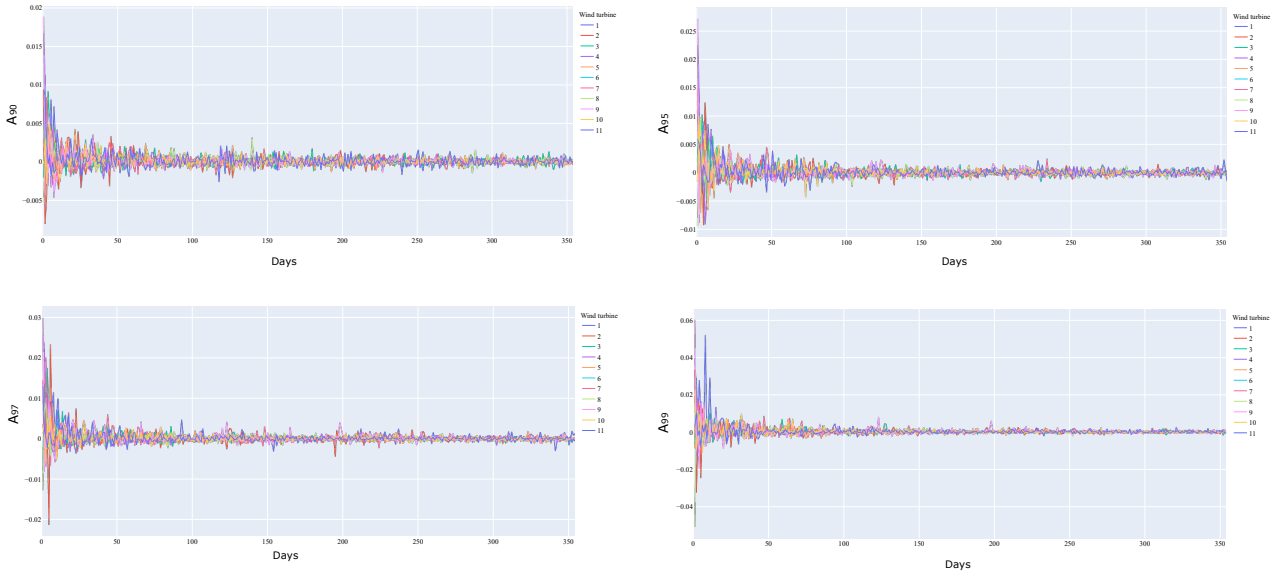

(**b**)

Figure 9. Temperature alarm thresholds converging over time. (**a**) generator bearing alarm convergence; (**b**) generator phase winding alarm convergence.

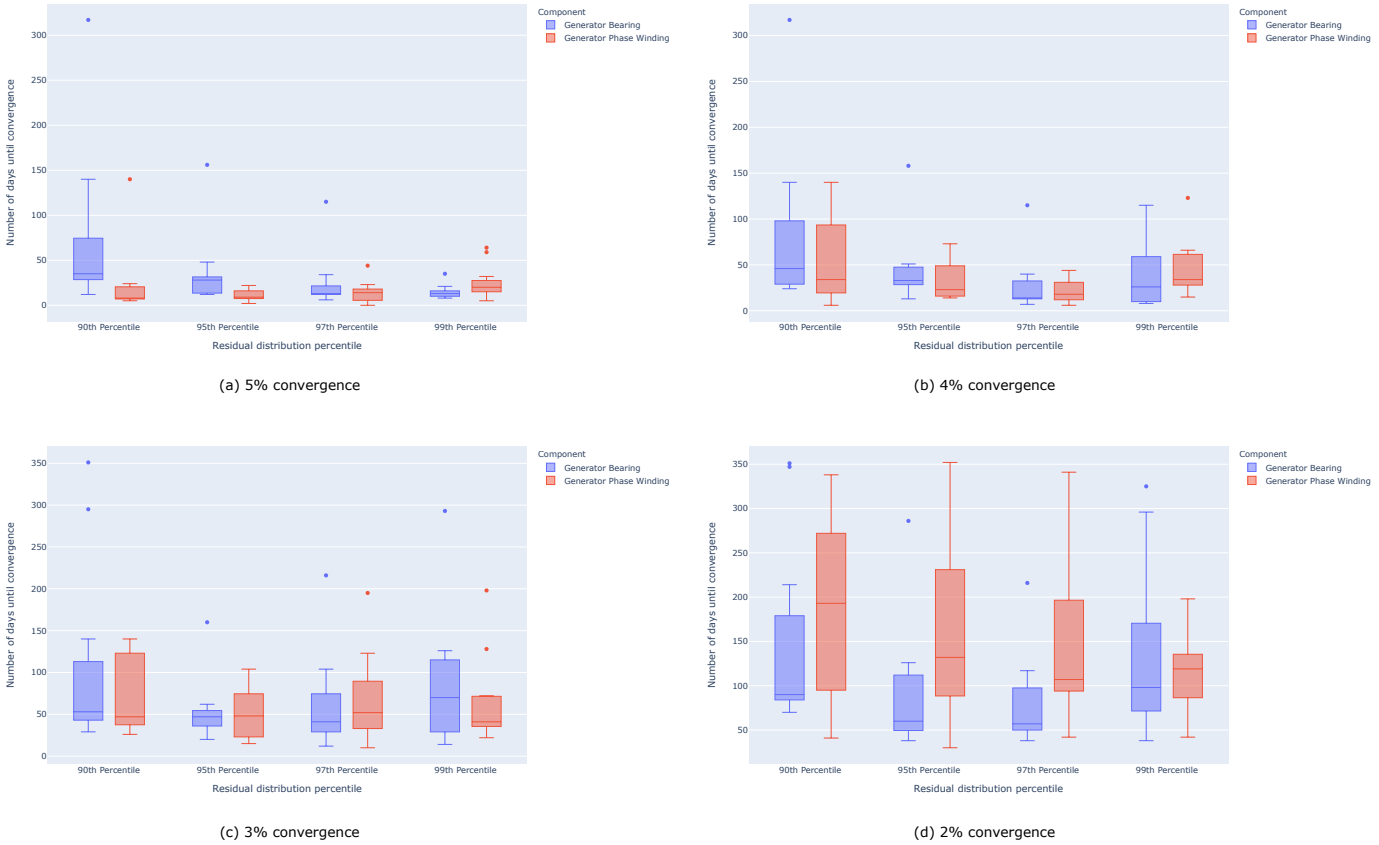

Figure 10. Convergence times.

4. Discussion and Conclusions

This work presented a comparative analysis of NBM temperature thresholds for generator bearings and phase windings. Four thresholds were utilised, each calculated from different percentiles of the temperature error residual distribution. For each temperature threshold, four convergence percentages were analysed to understand how much variability can be expected across components and turbines, as well as linking these to threshold convergence time to better understand how much data are required to produce robust alarms.

First of all, in terms of absolute residual alarm levels (measured temperature minus predicted temperature), results show that there is significantly more variation in the generator bearing temperature when compared to the phase winding temperature. This can be observed in Figure 3, and means that the input features used to create the NBM cannot explain the level of variance. This additional unexplained variance is transferred over to the alarm threshold through the NBM process, where lower performance in anomaly detection would be expected. Increasing accuracy of prediction would require a higher dimensional model with additional inputs that can further explain the observed relationship. In practice, this shows the importance of robust feature engineering, as different components do not always have the necessary inputs (and sensors) to create models of equal accuracy.

Regardless of modelling accuracy, a percentile can be chosen to reflect the residual error distribution. If we first of all consider 3%, 4% and 5% convergence (excluding 2% for now), the vast majority of turbines require less than 150 days to effectively train a stable threshold. In fact, if you eliminate the threshold based on the 90th percentile, the majority of turbines require less than 120 days, with the average being approximately 50–60 days. Only 1 or 2 significant outliers, each representing an individual turbine, lie outside this range. Once we move to 2% convergence criteria, the required data significantly increase, in some cases to include all available data, suggesting that the convergence criteria are

marginally too restrictive. In most cases, however (again excluding the threshold based on the 90th percentile), less than 250 days of data are required.

Finding the correct balance between minimising false alarms and accurately picking up anomalies can be difficult. Feature engineering to correctly identify and utilise features to create an accurate NBM is one part of the overall approach. Analysing and choosing the correct threshold based on NBM error residuals is equally as important. Results suggest that, on average, as little as two months of data are adequate to produce stable temperature alarm thresholds, with the worst case example requiring approximately 200–290 days of data depending on the component using a 3% convergence.

In practice, this suggests that initial models could be developed with a few months of data without the risk of increased false alarms and subsequent costly investigations. Once available, retraining the NBMs with up to 8–10 months of data would be recommended in order to further ensure alarm threshold convergence is achieved to minimise this risk.

Author Contributions: Conceptualization, A.T. and A.M.; methodology, A.T.; validation, A.T. ; formal analysis, A.T.; data curation, A.T. and J.C.; writing—original draft preparation, A.T.; writing—review and editing, A.T. and J.C.; visualization, A.T.; supervision, J.C. and A.M.; funding acquisition, J.C. All authors have read and agreed to the published version of the manuscript.

Funding: This research was funded by EPSRC Grant No. EP/T031549/1.

Institutional Review Board Statement: Not applicable.

Informed Consent Statement: Not applicable.

Conflicts of Interest: The authors declare no conflict of interest.

Abbreviations

The following abbreviations are used in this manuscript:

ANN	Artificial Neural Network
ARX	Auto-Regressive with eXogenous input
DFIG	Doubly-Fed Induction Generator
FSRC	Full Signal Reconstruction
MSE	Mean Squared Error
NARX	Nonlinear Auto-Regressive neural networks with eXogenous input
NBM	Normal Behaviour Model
RMSE	Root Mean Squared Error
SCADA	Supervisory Control and Data Acquisition

References

1. Tautz-Weinert, J.; Watson, S. Using SCADA data for wind turbine condition monitoring—A review. *IET Renew. Power Gener.* **2017**, *11*, 382–394.
2. Raschka, S.; Mirjalili, V. *Python Machine Learning*, 3rd ed.; Packt Publishing: Birmingham, UK, 2019.
3. Garlick, W.; Dixon, R.; Watson, S. A Model-Based Approach to Wind Turbine Condition Monitoring Using SCADA Data. 2009. Available online: https://repository.lboro.ac.uk/account/articles/9555557 (accessed on 9 May 2022).
4. Wilkinson, M.; Darnell, B.; Van Delft, T.; Harman, K. Comparison of methods for wind turbine condition monitoring with SCADA data. *IET Renew. Power Gener.* **2014**, *8*, 390–397. https://doi.org/10.1049/IET-RPG.2013.0318.
5. McArthur, S.; Catterson, V.; McDonald, J. A multi-agent condition monitoring architecture to support transmission and distribution asset management. In Proceedings of the 3rd IEE International Conference on Reliability of Transmission and Distribution Networks, 2005; pp. 87–91. London, UK, 15-17 Feb. 2005 https://doi.org/10.1049/cp:20050017.
6. Schlechtingen, M.; Ferreira Santos, I. Comparative analysis of neural network and regression based condition monitoring approaches for wind turbine fault detection. *Mech. Syst. Signal Process.* **2011**, *25*, 1849–1875. https://doi.org/10.1016/J.YMSSP.2010.12.007.
7. Zhang, Z.Y.; Wang, K.S. Wind turbine fault detection based on SCADA data analysis using ANN. *Adv. Manuf.* **2014**, *2*, 70–78. https://doi.org/10.1007/s40436-014-0061-6.
8. Verma, A.; Kusiak, A. Fault Monitoring of Wind Turbine Generator Brushes: A Data-Mining Approach. *J. Sol. Energy Eng.-Trans. Asme* **2012**, *134*, 9. https://doi.org/10.1115/1.4005624.

9. Yan, Y.; Li, J.; Gao, D.W. Condition Parameter Modeling for Anomaly Detection in Wind Turbines. *Energies* **2014**, *7*, 3104–3120. https://doi.org/10.3390/EN7053104.
10. Pei, Y.; Qian, Z.; Tao, S.; Yu, H. Wind Turbine Condition Monitoring Using SCADA Data and Data Mining Method. In Proceedings of the 2018 International Conference on Power System Technology, POWERCON 2018-Proceedings, Guangzhou, China, 6–9 November 2018; pp. 3760–3764. https://doi.org/10.1109/POWERCON.2018.8601803.
11. Bangalore, P.; Tjernberg, L.B. An Artificial Neural Network Approach for Early Fault Detection of Gearbox Bearings. *IEEE Trans. Smart Grid* **2015**, *6*, 980–987. https://doi.org/10.1109/TSG.2014.2386305.
12. Bangalore, P.; Letzgus, S.; Karlsson, D.; Patriksson, M. An artificial neural network-based condition monitoring method for wind turbines, with application to the monitoring of the gearbox. *Wind Energy* **2017**, *20*, 1421–1438. https://doi.org/10.1002/WE.2102.
13. Cui, Y.; Bangalore, P.; Tjernberg, L.B. An anomaly detection approach based on machine learning and scada data for condition monitoring of wind turbines. In Proceedings of the 2018 International Conference on Probabilistic Methods Applied to Power Systems, PMAPS 2018-Proceedings, Boise, ID, USA, 24–28 June 2018. https://doi.org/10.1109/PMAPS.2018.8440525.
14. Wang, Y.; Infield, D. Supervisory control and data acquisition data-based nonlinear state estimation technique for wind turbine gearbox condition monitoring. *IET Renew. Power Gener.* **2013**, *7*, 350–358. https://doi.org/10.1049/IET-RPG.2012.0215.
15. Qiu, Y.; Feng, Y.; Tavner, P.; Richardson, P.; Erdos, G.; Chen, B. Wind turbine SCADA alarm analysis for improving reliability. *Wind Energy* **2012**, *15*, 951–966. https://doi.org/10.1002/WE.513.
16. Jardine, A.K.; Lin, D.; Banjevic, D. A review on machinery diagnostics and prognostics implementing condition-based maintenance. *Mech. Syst. Signal Process.* **2006**, *20*, 1483–1510. https://doi.org/10.1016/J.YMSSP.2005.09.012.
17. Abouel-Seoud, S.A. Fault detection enhancement in wind turbine planetary gearbox via stationary vibration waveform data. *J. Low Freq. Noise Vib. Act. Control* **2017**, *37*, 477–494. https://doi.org/10.1177/1461348417725950.
18. Wu, G.X.; Zuo, Y.B.; Shi, Y.H. Research on Vibration Signal Feature Extraction Method to the Wind Turbine Generator. *Adv. Mater. Res.* **2014**, *902*, 370–377. https://doi.org/10.4028/WWW.SCIENTIFIC.NET/AMR.902.370.
19. Mollasalehi, E. Data-Driven and Model-Based Bearing Fault Analysis—Wind Turbine Application. Ph.D. Thesis, University of Calgary, Calgary, AB, Canada, 2017.
20. Kim, S.; An, D.; Choi, J.H. Diagnostics 101: A Tutorial for Fault Diagnostics of Rolling Element Bearing Using Envelope Analysis in MATLAB. *Appl. Sci.* **2020**, *10*, 7302. https://doi.org/10.3390/APP10207302.
21. Turnbull, A.; Carroll, J.; Koukoura, S.; McDonald, A. Prediction of wind turbine generator bearing failure through analysis of high-frequency vibration data and the application of support vector machine algorithms. *J. Eng.* **2019**, *2019*, 4965–4969. https://doi.org/10.1049/joe.2018.9281.
22. Ogata, J.; Murakawa, M. Vibration-Based Anomaly Detection Using FLAC Features for Wind Turbine Condition Monitoring. In Proceedings of the 8th European Workshop On Structural Health Monitoring, Bilbao, Spain, 5–8 July 2016.
23. Koukoura, S.; Carroll, J.; McDonald, A.; Weiss, S. Comparison of wind turbine gearbox vibration analysis algorithms based on feature extraction and classification. *IET Renew. Power Gener.* **2019**, *13*, 2549–2557. https://doi.org/10.1049/IET-RPG.2018.5313.
24. Koukoura, S.; Carroll, J.; McDonald, A. On the use of AI based vibration condition monitoring of wind turbine gearboxes. *J. Phys. Conf. Ser.* **2019**, *1222*, 012045. https://doi.org/10.1088/1742-6596/1222/1/012045.
25. Tsui, K.L.; Chen, N.; Zhou, Q.; Hai, Y.; Wang, W. Prognostics and health management: A review on data driven approaches. *Math. Probl. Eng.* **2015**, *2015*, 793161. https://doi.org/10.1155/2015/793161.
26. Liu, R.; Yang, B.; Zio, E.; Chen, X. Artificial intelligence for fault diagnosis of rotating machinery: A review. *Mech. Syst. Signal Process.* **2018**, *108*, 33–47. https://doi.org/10.1016/j.ymssp.2018.02.016.
27. Stetco, A.; Dinmohammadi, F.; Zhao, X.; Robu, V.; Flynn, D.; Barnes, M.; Keane, J.; Nenadic, G. Machine learning methods for wind turbine condition monitoring: A review. *Renew. Energy* **2019**, *133*, 620–635. https://doi.org/10.1016/j.renene.2018.10.047.